This is the author's final, peer-reviewed manuscript as accepted for publication. The publisher-formatted version may be available through the publisher's web site or your institution's library.

Expansion of human mesenchymal stem cells in a fixed-bed bioreactor system based on non-porous glass carrier – Part B: Modeling and scale-up of the system

Christian Weber, Denise Freimark, Ralf Pörtner, Pablo Pino-Grace, Sebastian Pohl, Christine Wallrapp, Peter Geigle, Peter Czermak

How to cite this manuscript (APA format)

If you make reference to this version of the manuscript, use the following citation format:

Weber, C., Freimark, D., Pörtner, R., Pino-Grace, P., Pohl, S., Wallrapp, C., Geigle, P., Czermak, P. (2010). Expansion of human mesenchymal stem cells in a fixed-bed bioreactor system based on non-porous glass carrier – Part B: Modeling and scale-up of the system. Retrieved from http://krex.ksu.edu

Published Version Information

Citation: Weber, C., Freimark, D., Pörtner, R., Pino-Grace, P., Pohl, S., Wallrapp, C., Geigle, P., Czermak, P. (2010). Expansion of human mesenchymal stem cells in a fixed-bed bioreactor system based on non-porous glass carrier – Part B: Modeling and scale-up of the system. International Journal of Artificial Organs, 33 (11), 782-795.

Copyright: **The International Journal of Artificial Organs** is published and copyrighted by Wichtig Editore - Milano (Italy)

Digital Object Identifier (DOI):

Publisher's Link: http://www.artificial-organs.com/public/IJAO/Issue/Issue.aspx?UidIssue=6075300D-381E-4BE5-98FC-22498D389E15

This item was retrieved from the K-State Research Exchange (K-REx), the institutional repository of Kansas State University. K-REx is available at http://krex.ksu.edu

Expansion of human mesenchymal stem cells in a fixed-bed bioreactor system based on non-porous glass carrier – Part B: Modeling and scale up of the system

Short title: Expansion of hMSC-TERT in a fixed-bed bioreactor – Part B

Christian Weber
Institute of Biopharmaceutical Technology, University of Applied Sciences Giessen-Friedberg, Giessen, Germany

Denise Freimark
Institute of Biopharmaceutical Technology, University of Applied Sciences Giessen-Friedberg, Giessen, Germany

Ralf Pörtner
Institute of bioprocess and Biosystems Engineering, University of Technology, Hamburg, Germany

Pablo Pino-Grace
Institute of Biopharmaceutical Technology, University of Applied Sciences Giessen-Friedberg, Giessen, Germany

Sebastian Pohl
Institute of Biopharmaceutical Technology, University of Applied Sciences Giessen-Friedberg, Giessen, Germany

Christine Wallrapp
CellMed AG, Alzenau, Germany

Peter Geigle
CellMed AG, Alzenau, Germany

Peter Czermak

Institute of Biopharmaceutical Technology, University of Applied Sciences Giessen-Friedberg, Giessen, Germany
Department of Chemical Engineering, Kansas State University, Manhattan KS, USA

Corresponding author: Peter Czermak; Wiesenstraße 14, 35390 Giessen, Germany, phone +496413092634, fax +496413092553, e-mail peter.czermak@tg.fh-giessen.de

Abstract

Human mesenchymal stem cells (hMSC) are a promising cell source for the manufacturing of cell therapeutic or tissue engineered implants. In part A of this publication a fixed-bed bioreactor system based on non-porous borosilicate glass spheres and procedures for the automated expansion of hMSC with high yield and vitality has been introduced. Part B of this study deals with the modeling of the process in order to transfer the bioreactors system from the laboratory to the production scale. Relevant model parameters have been obtained by fitting them to the experimental data of hMSC-TERT cultivations in scales up to 300 cm^3. Scale-up calculations were carried out exemplarily for a target cell number of twenty billion cells.

Key words

mesenchymal stem cells, hMSC-TERT, fixed-bed bioreactor, glass carrier, scale up

Introduction

Human mesenchymal stem cells (hMSC) or allogenic stem-cell lines are a promising cell source for the manufacturing of cell therapeutic implants such as microencapsulated hMSC-TERT for the treatment of diabetes mellitus or stroke [1, 2]. The expansion of the initial cell number to a relevant scale, especially for producing of at all times available implants in stock, demands an automatable and scalable bioreactor system which offers a gentle cultivation and harvesting of the cells. For that purpose a fixed bed bioreactor system based on non-porous borosilicate glass spheres with a diameter of 2 mm as well as inoculation, cultivation, and harvesting procedures, which fulfills the requirements stated above were introduced in part A of this publication [3] . It could be shown in previous studies that the chosen carriers are most suitable in respect to the nutrient supply and harvesting behavior [4]. Cultivations were performed in laboratory scales of up to 300 cm^3 (Table 1) in order to develop the automatable expansion process. The model cell line hMSC-TERT was used throughout the experiments [5]. The developed inoculation procedure consists of the filling of the fixed bed with cell suspension and repeated perfusion steps (7 min with and 30 min without perfusion). Applying this procedure four times resulted in a yield of adhered cells of about 50%. A vitality of 97% and a yield of harvested cells of 82% could be reached by perfusion of the fixed bed with Accutase™-solution in order to detach the cells from the carrier followed by flushing them out with the medium flow. The mean growth and consumption rates, calculated in a simplified manner (Table 2), are comparable to those published for stem cells and other animal cell types. Additional cultivations in 6-well cell culture plates were performed in order to determine the Monod kinetics of the growth and glucose consumption under static conditions (Table 5).

The cultivations, introduced in part A of this publication, were used in this part to obtain the constants of the growth and consumption kinetics of the below-mentioned model by fitting them to the experimental data (Table 1)[3]. These parameters allowed in combination with the mathematical model scale-up calculations. In order to establish a practical relationship, the system was exemplarily scaled for the cultivation of 20 billion cells, which are sufficient for the production of about 200 single doses of CellBeads® (CellMed AG, Alzenau, Germany). CellBeads® are therapeutic implants, which are currently in a clinical phase II study for the treatment

of stroke and consist of about 2000 to 2500 alginate encapsulated and genetically modified hMSC-TERT [1, 4, 6].

Model equations

The following assumptions and simplifications for modeling of the fixed bed process were made:

- homogenous but time dependent concentration profile in the conditioning vessel
- concentration profile in the fixed bed varies in time and axial direction
- radial gradients are negligible due to plug flow and a homogenous cell distribution in radial direction
- radial porosity profile is neglected
- convective and dispersive mass transport
- constant dispersion coefficient over the fixed bed region
- the growth rate depends on the glucose concentration (Monod-kinetic) and is independent from the oxygen concentration
- no cell lysis or apoptosis
- Monod kinetic for glucose and zero order kinetic for oxygen consumption
- isothermal conditions (37°C)
- laminar flow (Re < 10)

Since glutamine was reported as an unimportant energy source for hMSC only the oxygen and glucose kinetics were taken into account [7].

Figure 1 gives an overview of the model, which considers the mass balance of the conditioning vessel and the fixed bed.

The temporally and spatial concentration profile c_i of nutrient i in the fixed bed can be described by a steady state convection-dispersion-reaction equation:

$$\varepsilon \cdot \frac{\delta c_i}{\delta t} = -v \cdot \frac{\delta c_i}{\delta z} + D_{ax} \cdot \frac{\delta^2 c_i}{\delta z^2} - q_i \cdot X_{FB} \qquad \text{Equation 1}$$

with the Danckwerts boundary condition for the inlet and outlet boundary:

$$v \cdot c_{i,CV} = v \cdot c_i\big|_{z=0} - D_{ax} \cdot \frac{dc_i}{dz}\bigg|_{z=0}$$ Equation 2

$$\frac{dc_i}{dz}\bigg|_{z=h_{FB}} = 0$$ Equation 3

D_{ax} is the axial dispersion coefficient, ε the porosity, q_i the consumption rate, v the superficial velocity, $\dot{V}$ the volume flow, and X_{FB} the volume specific cell density. Cell growth during the exponential phase can be expressed as a first order kinetic:

$$\frac{dX_{FB}}{dt} = X_{FB} \cdot \mu$$ Equation 4

The growth rate μ depends on the glucose concentration $c_{Glc}\big|_{r=R}$ at the carrier surface according to a Monod kinetic:

$$\mu = \mu_{\max} \frac{c_{Glc}\big|_{r=R}}{c_{Glc}\big|_{r=R} + K_{M,\mu}}$$ Equation 5

The glucose consumption rate q_{Glc} is also a function of the glucose concentration $c_{Glc}\big|_{r=R}$:

$$q_{Glc} = q_{Glc,\max} \cdot \frac{c_{Glc}\big|_{r=R}}{c_{Glc}\big|_{r=R} + K_{M,q_{Glc}}}$$ Equation 6

whereas the oxygen uptake rate q_{Ox} is regarded as independent from the concentration and thus constant:

$$q_{Ox} = const.$$ Equation 7

For calculation of the concentration $c_i\big|_{r=R}$ at the carrier surface a diffusive mass transfer through the hydrodynamic boundary layer is assumed, which is in equilibrium with the nutrient consumption of the cells at the carrier surface (Figure 2):

$$\frac{\dot{N}_i}{A} = k_{l,i} \cdot (c_i - c_i\big|_{r=R}) = X_A \cdot q_i \qquad \text{Equation 8}$$

The mass transfer coefficient $k_{l,i}$ can be calculated by a Sherwood relation [8]:

$$Sh = \frac{k_{l,i} \cdot d}{D_{i,M}} = 4,58 \cdot \mathrm{Re}^{1/3} \cdot Sc^{1/3} \qquad \text{Equation 9}$$

with the Schmidt and Reynolds number:

$$Sc = \frac{\eta}{D_{i,M} \cdot \rho} \qquad \text{Equation 10}$$

$$Re = \frac{v \cdot \rho \cdot d}{\eta} \qquad \text{Equation 11}$$

$D_{i,M}$ is the molecular diffusion coefficient of the nutrient i and η and ρ are the viscosity and density of the medium, respectively.

The time dependent change in glucose content in the conditioning vessel is composed of the flux $\dot{V} \cdot c_{i,FB}$ from the fixed bed to the conditioning vessel and the flux $\dot{V} \cdot c_{i,CV}$ out of the conditioning vessel to the fixed bed (Figure 1):

$$V_{CV} \cdot \frac{dc_{Glc,CV}}{dt} = \dot{V} \cdot c_{Glc,FB} - \dot{V} \cdot c_{Glc,CV} \qquad \text{Equation 12}$$

In the case of oxygen an additional term, the oxygen transfer rate OTR, arises:

$$V_{CV} \cdot \frac{dc_{Ox,CV}}{dt} = \dot{V} \cdot c_{Ox,FB} - \dot{V} \cdot c_{Ox,CV} + OTR$$ Equation 13

The oxygen transfer rate can be calculated with the volumetric oxygen transfer coefficient $k_l a$ and the maximal oxygen saturation c^*_{Ox}:

$$OTR = k_l a \cdot V_{CV} \cdot (c^*_{Ox} - c_{Ox,CV})$$ Equation 14

Methods

The cultivations in scales of up to 300 cm^3 were performed as previously described in part A of this publication (Table 1) [3]. Following model parameters were fitted to the experimental data:

- initial cell density X_{FB}^{0} (differs from inoculated cell density)
- maximal glucose uptake rate $q_{Glc,\max}$
- Monod constant for glucose uptake kinetic $K_{M,q_{Glc}}$
- oxygen uptake rate q_{Ox}
- maximal growth rate $\mu_{\max}$
- Monod constant for growth kinetic $K_{M,\mu_{Glc}}$
- volumetric oxygen transfer rate $k_l a$

The superficial velocity was restricted to 3 x 10^{-4} m s^{-1} by using of the mean growth rate as indicator (see part A) [3]. Since the maximal superficial velocity is restricted, the fixed bed height h_{FB} depends mainly on the target cell density X_{FB}^{n} and the minimal tolerable oxygen saturation of the medium. The lowest oxygen saturation $s_{Ox,FB}$ can be found in the outlet region. The inflow was presumed to be saturated with normal air (approx. 20% oxygen) that means a concentration of dissolved oxygen of 6.88 µg mL^{-1}. The defined fixed bed height h_{FB} allowed a calculation of the thickness-ratio TR dependent maximal fixed-bed volume and thus the scaling of a single fixed-bed:

$$V_{FB} = h_{FB} \cdot \pi \cdot \left(\frac{h_{FB}}{TR \cdot 2} \right)^2$$

Equation 15

A further up-scaling of the reactor system can only be performed by increasing the number of parallel operated fixed-beds n_{FB}. The number n_{FB} needed for the target cell number N_X^n can be calculated as follows:

$$n_{FB} = \frac{N_X^n}{X_{FB}^n \cdot V_{FB}}$$

Equation 16

Simulations of the up-scaled cultivation process were performed with selected parameter settings (Table 7).

Results and Discussion

The cell line hMSC-TERT was cultured in scales of 14, 60, and 300 cm^3. Figure 3 to Figure 5 show the experimental data as well as the according simulated curves. The results are summarized in Table 5.

Most model parameters of the cultivation in the 14.2- and 60-cm^3 fixed-bed reactors (passage number 68 and 71) are comparable to those obtained in 6-well cell culture plates (passage number 69) or at least within the two sigma range. The plausibility of the fitted parameters and thus of the model by itself can be confirmed by the mean growth and consumption kinetics obtained with the simplified calculations without consideration of concentration dependencies and mass transfer resistances (Table 2 and part A) [3]. All kinetics are in the range of those reported for several animal and human cells or cell lines (see part A and Table 4).

The cells were cultured up to a density X_{FB}^{n} of (2.93 ± 0.11) x 10^6 cells/cm^3. Higher cell densities are not recommendable because of the risk of channeling and drawbacks by up-scaling of the fixed bed system as shown below. The initial cell densities X_{FB}^{0} (X_{A}^{0}) were about 50% of the inoculated cell densities that confirms the results of the inoculation procedure in part A [3].

The maximal growth rate $\mu_{\max}$ and the oxygen consumption rate q_{Ox} decreased with advancing passage number from 0.69 to 0.55 d^{-1} and 2.14 x 10^{-8} to about 1.1 x 10^{-8} mg h^{-1} $cell^{-1}$. The maximal glucose consumption rate $q_{Glc,\max}$ increased from 8.0 x 10^{-8} to 11.8 x 10^{-8} mg h^{-1} $cell^{-1}$. As a consequence of these changes in growth and consumption kinetics process optimizations and scale up calculations are only valid for a closed range of passage numbers.

When a fixed superficial velocity v and an oxygen saturation $s_{Ox,CV}$ of 100% at the inlet is assumed, the maximal fixed bed height h_{FB} is a function mainly of the cell density X_{FB} and the minimal oxygen saturation in the fixed bed $s_{Ox,FB}$, which can be found as already mentioned at the outlet region. Thus the feasible fixed bed height decreases with increasing outlet oxygen saturation and cell density. By using Equation 15 and Equation 16 one obtains the numbers and volumes of parallel

operated fixed-bed reactors needed for the exemplified cultivation of twenty billion cells as a function of the thickness ratio TR, outlet oxygen saturation $s_{Ox,FB}$, and cell density at the end of cultivation X_{FB}^{n} (Table 6). For example, a thickness ratio of three, an outlet oxygen saturation of 40% as well as a cell density of 3.66 x 10^6 cells/cm^3 means a maximal volume of a single bed of 17 cm^3 and because of this small fixed bed volume a number of 312 parallel operated reactors. This is very unpractical in handling and operating. Thus, it is recommended to reduce the thickness ratio, cell density, and to an uncritical value, the outlet oxygen saturation. Indeed this leads to an increase of the total fixed bed volume but reduces the number of needed reactors due to a greater volume of a single fixed bed. For instance a cell density of 9.15 x 10^5 cells/cm^3, a thickness ratio of one, and an oxygen saturation at the outlet of 20% result in a single reactor of about 22 Liters. This is a considerable decrease in complexity of the reactor system for the cultivation of twenty billion hMSC-TERT.

The dissolved oxygen saturation at the carrier surface $s_{Ox}\big|_{r=R}$ differs slightly from those of the bulk medium due to the mass transfer resistance of the hydrodynamic boundary layer (Figure 2). This difference increases with increasing cell density.

A positive effect of hypoxic conditions on the proliferation rate and maintenance of the undifferentiated state was described in several publications [9-13]. Additionally it could be shown that mesenchymal stem cells, which had been cultured under hypoxic conditions (2 - 5% oxygen in the aeration gas) showed a better differentiation potential when transferred to normoxic conditions [10, 11]. It could be gathered from this that an oxygen saturation of 20% is sufficient or even supportive for the expansion cultivation and could be, when indicated, more reduced. However, this demands further investigations.

Figure 8 shows the glucose concentration in the medium c_{Glc} versus the cell density X_{FB} for maintaining some presetted growth rates μ, which depend on the glucose concentration at the carrier surface $c_{Glc}\big|_{r=R}$. The effect of the cell density is insignificant at least in the presented range of up to 4.6 x 10^6 cells/cm^3 and a minimal glucose saturation in the medium of 0.135 mg mL^{-1}. This speaks for a negligible mass transfer resistance for glucose despite of a smaller mass transfer coefficient compared to those of oxygen. This can be explained by the fact that the glucose

concentration and thus the driving force for the mass transfer is of magnitudes greater.

Four simulations at a twenty-billion-cells scale with several combinations of initial and target cell densities as well as minimal oxygen saturation at the outlet and medium volume in the conditioning vessel were performed exemplarily (Table 7). The results of these simulations are shown in Table 8. The simulations 1 and 4 are shown graphically in Figure 9 and Figure 10.

The longest cultivation time of 233 h shows simulation 4. This is mainly due to the small initial density X_{FB}^{0} of 1.83 x 10^4 cell/cm^3 (1000 cells/cm^2). This low initial cell density and the target cell density X_{FB}^{n} of 1.83 x 10^6 cell/cm^3 means an amplification of the initial cell number of the factor 100. The amplification factor of the simulations 1 to 3 is only 20. Considering the yield of adherent cells after the inoculation procedure of about 50% and the yield as well as vitality after the harvesting procedure of 82% and 96%, respectively, the efficiency of the cultivation is additionally lowered. The amplification factor of the simulation 1 to 3 is then 7.9 and those of the simulation 4 of about 40. For enhancing of the overall yield of the cultivation process, the initial cell density can be reduced or the target cell density can be increased. The latter would lead, as already discussed, to a higher number of parallel operated fixed beds and thus to an increased complexity of the system. A small initial cell density can enhance the growth rate but stretches the lag-phase [14, 15]. Moreover the cells would growth in clusters which has some drawbacks concerning the harvest procedure and nutrient supply. A compromise has to be found between the two possibilities reduction of the initial cell density or enhancement of the target cell density. Furthermore the inoculation procedure has to be optimized in order to reduce the needed inoculum.

Since the growth rate depends on the glucose concentration the cultivation time of up to 233 h can be reduced by increasing of the medium volume and thus the glucose mass. But this would mean a suboptimal exploitation of the medium. The medium should be added step wise to the process and stored at 4°C in order to avoid a degradation of thermolabile components.

The greatest difference between the glucose concentration c_{Glc} at the inlet and outlet is 0.022 mg/mL or 7.5%, respectively (simulation 1). This has to be considered by measuring the glucose concentration for process monitoring in the conditioning

vessel. Due to the low solubility of oxygen the decrease in axial direction is with 70% to 80% much greater, which means a permanent aeration of the medium in the conditioning vessel in order to obtain an oxygen-saturated inflow of the fixed bed. The relative difference between the glucose concentration in the medium c_{Glc} and at the carrier surface $c_{Glc}\big|_{r=R}$ at the end of the cultivation is smaller than 0.8% and can be neglected just as the oxygen difference between the medium and carrier surface, which is of about 1 - 2%, dependent on the cell density.

Conclusion

A fixed-bed bioreactor system based on non-porous borosilicate glass carrier for the expansion of hMSC-TERT or hMSC and a scale-up procedure is introduced in this experimental and modeling study. The scalable fixed bed enables the expansion and harvesting of hMSC with high yield and vitality and offers an easy automation of the entire process including the inoculation, cultivation, and harvesting procedure (see part A of this publication) [3].

Scale-up calculations based on the experimentally determined oxygen consumption of the cells have revealed that reaching as much as possible high target cell densities is counterproductive in scaling of the process. Assuming a limited superficial velocity, the volume of a single fixed bed drastically decreases with increasing cell density, oxygen outlet concentration, and thickness ratio. This means a great number of parallel operated fixed beds and thus an enhanced complexity of the system. Therefore, it is recommendable to decrease the cell density as well as the thickness ratio and, certainly only to an uncritical value, the minimal oxygen saturation at the outlet. This leads to a reduction of the fixed bed number and thus simplifies the up-scaled system.

Appendix

Determination of the axial dispersion coefficient

For experimental determination of the axial dispersion coefficient in equation Equation 1 and Equation 2 a step function using ethylene violet stained water was applied at the inlet of the fixed-bed reactor, which then displaced the unstained water. Samples were taken at the outlet and the extinction as a measure for the concentration was determined photometrically. The normalized concentrations C were plotted against the normalized times $\theta = t / \mathrm{T}$, where T is the mean residence time in the fixed-bed reactor. The Bodenstein number

$$Bo = \frac{v \cdot h_{FB}}{D_{ax}} \qquad \text{Equation 17}$$

which contains the axial dispersion coefficient D_{ax} was then calculated by fitting the dimensionless convection-dispersion equation

$$\frac{\delta C}{\delta \theta} = -\frac{\delta C}{\delta Z} + \frac{1}{Bo} \cdot \frac{\delta^2 C}{\delta Z^2} \qquad \text{Equation 18}$$

to the experimental data. The boundary conditions were given by:

$$C\big|_{Z=0^-} = C\big|_{Z=0^+} - \frac{1}{Bo} \cdot \frac{\delta C}{\delta Z}\bigg|_{Z=0^+} \qquad \text{Equation 19}$$

$$\frac{\delta C}{\delta Z}\bigg|_{Z=1} = 0 \qquad \text{Equation 20}$$

An overview of examined fixed bed dimensions and superficial velocities is given in table Table 9.

Nomenclature

A	Growth surface [m^2]
Bo	Bodenstein number [-]
C	dimensionless concentration [-]
c_{Glc}^{0}	initial glucose concentration [kg m^{-3}]
c_{Glc}	glucose concentration in the fixed bed [kg m^{-3}]
$c_{Glc,CV}$	glucose concentration in the conditioning vessel (fixed-bed inlet) [kg m^3]
$c_{Glc,FB}$	glucose concentration in the fixed-bed outlet [kg m^3]
c_i	concentration of nutrient i [kg m^{-3}]
$c_{i,FB}$	concentration of nutrient i in the fixed-bed outlet [kg m^{-3}]
$c_{i,CV}$	concentration of nutrient i in the conditioning vessel [kg m^{-3}]
c_{Ox}^{*}	maximal dissolved oxygen [kg m^{-3}]
$c_{Ox,CV}$	oxygen concentration in the conditioning vessel (fixed-bed inlet) [kg m^3]
$c_{Ox,FB}$	oxygen concentration in the fixed-bed outlet [kg m^3]
d	sphere diameter [m]
D_{ax}	axial dispersion coefficient [m^2 s^{-1}]
$D_{i,M}$	molecular diffusion coefficient of nutrient i [m^2 s^{-1}]
h_{FB}	fixed bed height [m]
hMSC	human mesenchymal stem cells
$k_l a$	volumetric oxygen transfer coefficient [s^{-1}]

$k_{l,i}$	mass transfer coefficient [m s^{-1}]
$K_{M,\mu}$	Monod constant for growth kinetic [kg m^{-3}]
$K_{M,q_{Glc}}$	Monod constant for glucose consumption [kg m^{-3}]
n_{FB}	number of parallel operated fixed beds [-]
$\dot{N}$	mass flow rate [kg s^{-1}]
N_X^n	cell number at the end of cultivation [-]
OTR	oxygen transfer rate [kg m^{-3} s^{-1}]
q_{Glc}	glucose consumption rate [kg s^{-1} $cell^{-1}$]
$q_{Glc,\max}$	maximal glucose consumption rate [kg s^{-1} $cell^{-1}$]
q_i	consumption rate of nutrient i [kg s^{-1} $cell^{-1}$]
q_{Ox}	oxygen consumption rate [kg s^{-1} $cell^{-1}$]
Re	Reynolds number [-]
Sc	Schmidt number [-]
Sh	Sherwood number [-]
$s_{Ox,FB}$	oxygen saturation in the fixed-bed outlet [%]
$s_{Ox,CV}$	oxygen saturation in the conditioning vessel (fixed-bed inlet) [%]
TR	thickness ratio [-]
v	superficial velocity [m s^{-1}]
V	volume [m^3]
$\dot{V}$	flow rate [m^3 s^{-1}]

V_{FB}	fixed bed volume [m^3]
V_{CV}	medium volume (conditioning vessel) [m^3]
X_A	area related cell density [m^{-2}]
X_{FB}	volume related cell density [m^3]
X_{FB}^0	initial volume related cell density [m^3]
X_{FB}^n	volume related cell density at the end of cultivation [m^{-3}]
Z	dimensionless z-coordinate [-]
Δt^j	time intervall $t^j - t^{j-1}$ j = 1, 2, 3 … n
ε	void volume of the fixed bed (porosity) [-]
η	dynamic viscosity [Pa s]
μ	growth rate [s^{-1}]
μ_{max}	maximal growth rate [s^{-1}]
ρ	density of the medium [kg m^3]
θ	dimensionless time [-]
T	mean residence time [s]

Acknowledgements

The authors would like to thank the Federal ministry of Economics and Technology for financial support as well as the CellMed AG for providing the production cell line hMSC-TERT.

Figures

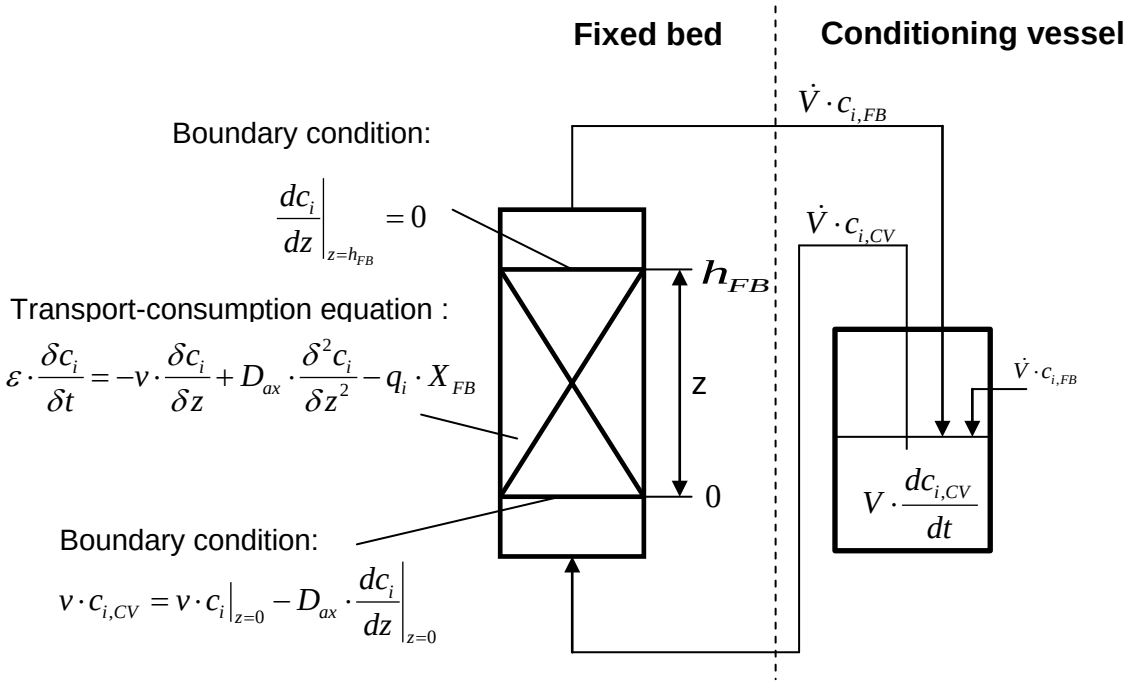

Figure 1

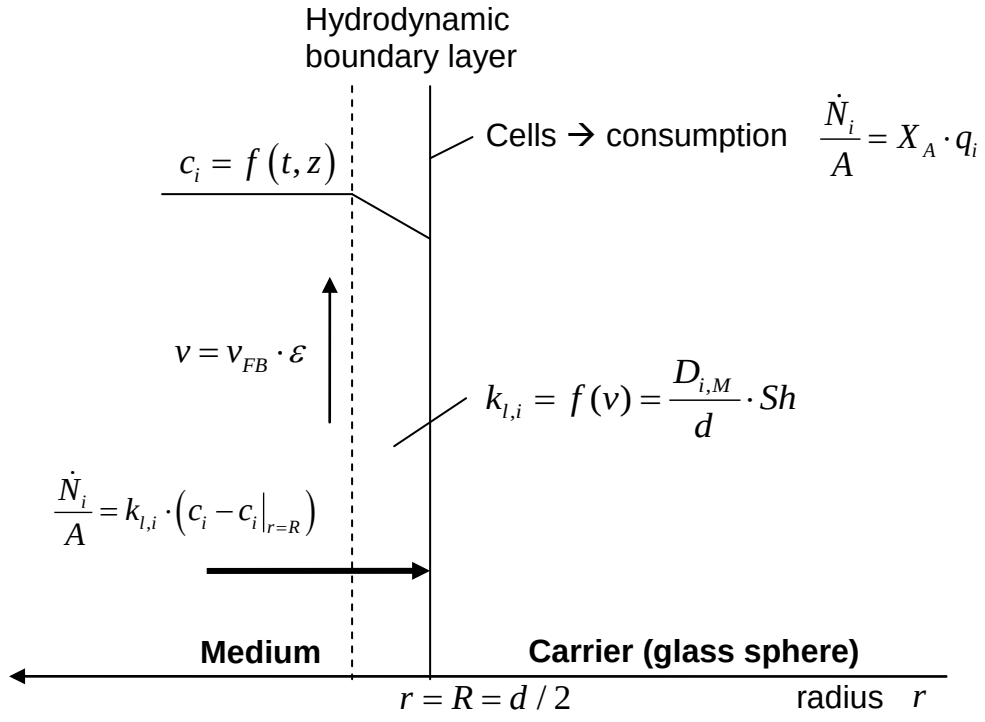

Figure 2

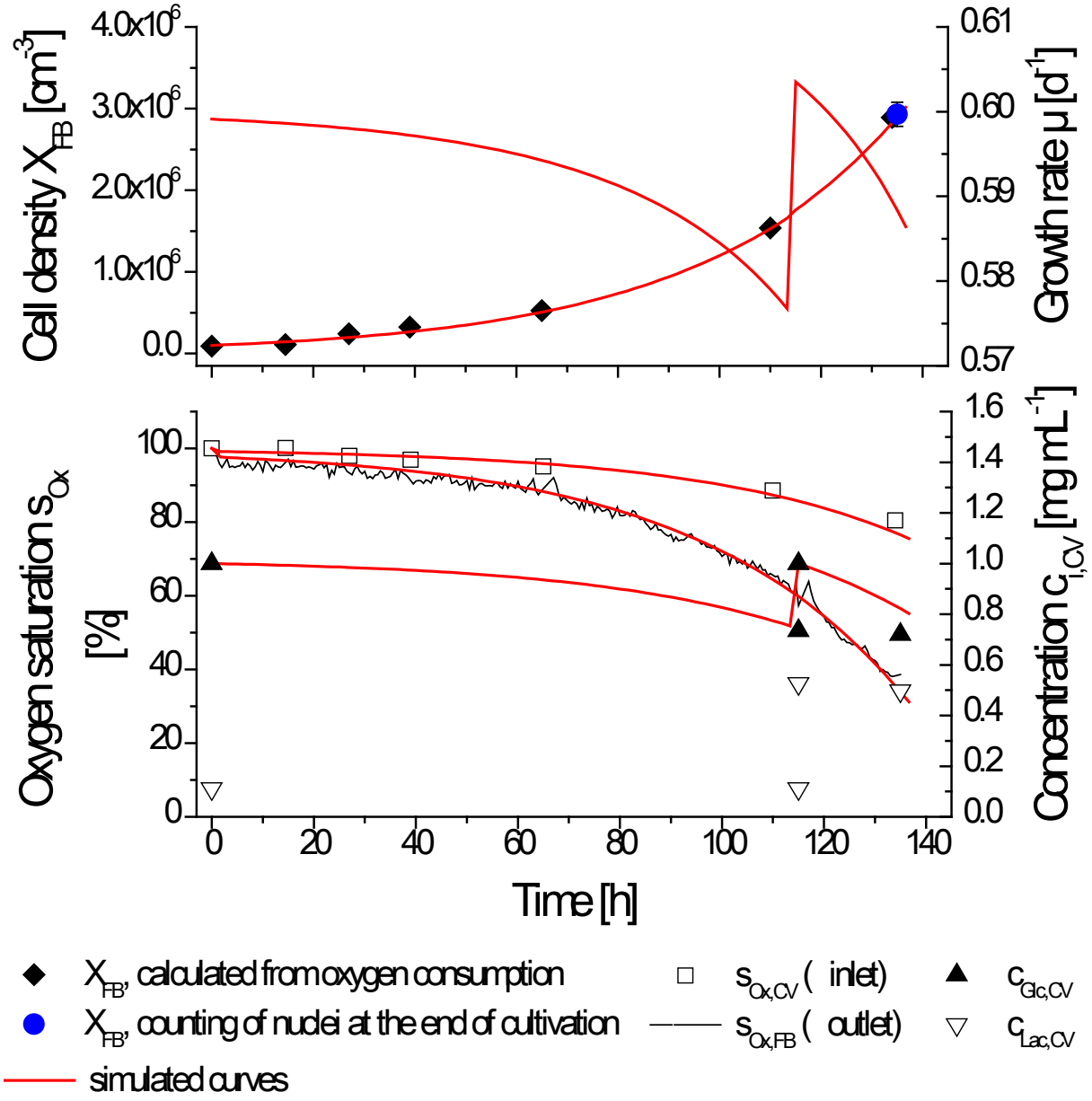
Cell density X_{FB} [cm^{-3}]
4.0x10^6
3.0x10^6
2.0x10^6
1.0x10^6
0.0
0.61
0.60
0.59
0.58
0.57
Growth rate μ [d^{-1}]
Oxygen saturation s_{Ox} [%]
100
80
60
40
20
0
1.6
1.4
1.2
1.0
0.8
0.6
0.4
0.2
0.0
Concentration $c_{i,CV}$ [mg mL^{-1}]
0
20
40
60
80
100
120
140
Time [h]
X_{FB}, calculated from oxygen consumption
X_{FB}, counting of nuclei at the end of cultivation
simulated curves
$s_{Ox,CV}$ (inlet)
$s_{Ox,FB}$ (outlet)
$c_{Glc,CV}$
$c_{Lac,CV}$

Figure 3

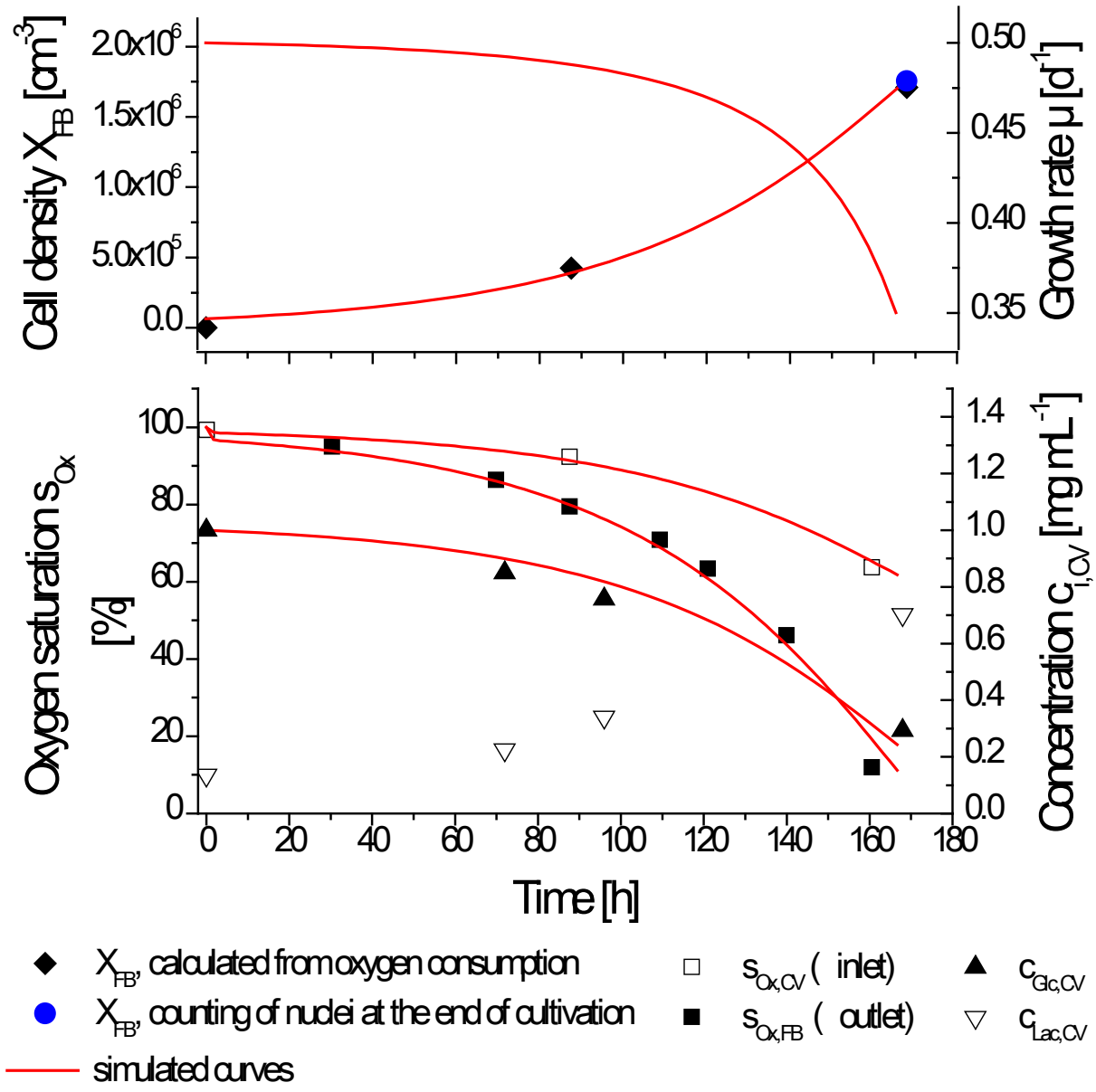
Cell density X_{FB} [cm^{-3}]
2.0x10^6
1.5x10^6
1.0x10^6
5.0x10^5
0.0
0.50
0.45
0.40
0.35
Growth rate μ [d^{-1}]
Oxygen saturation s_{Ox} [%]
100
80
60
40
20
0
1.4
1.2
1.0
0.8
0.6
0.4
0.2
0.0
Concentration $c_{i,CV}$ [mg mL^{-1}]
0
20
40
60
80
100
120
140
160
180
Time [h]
X_{FB}, calculated from oxygen consumption
X_{FB}, counting of nuclei at the end of cultivation
simulated curves
$s_{Ox,CV}$ (inlet)
$s_{Ox,FB}$ (outlet)
$c_{Glc,CV}$
$c_{Lac,CV}$

Figure 4

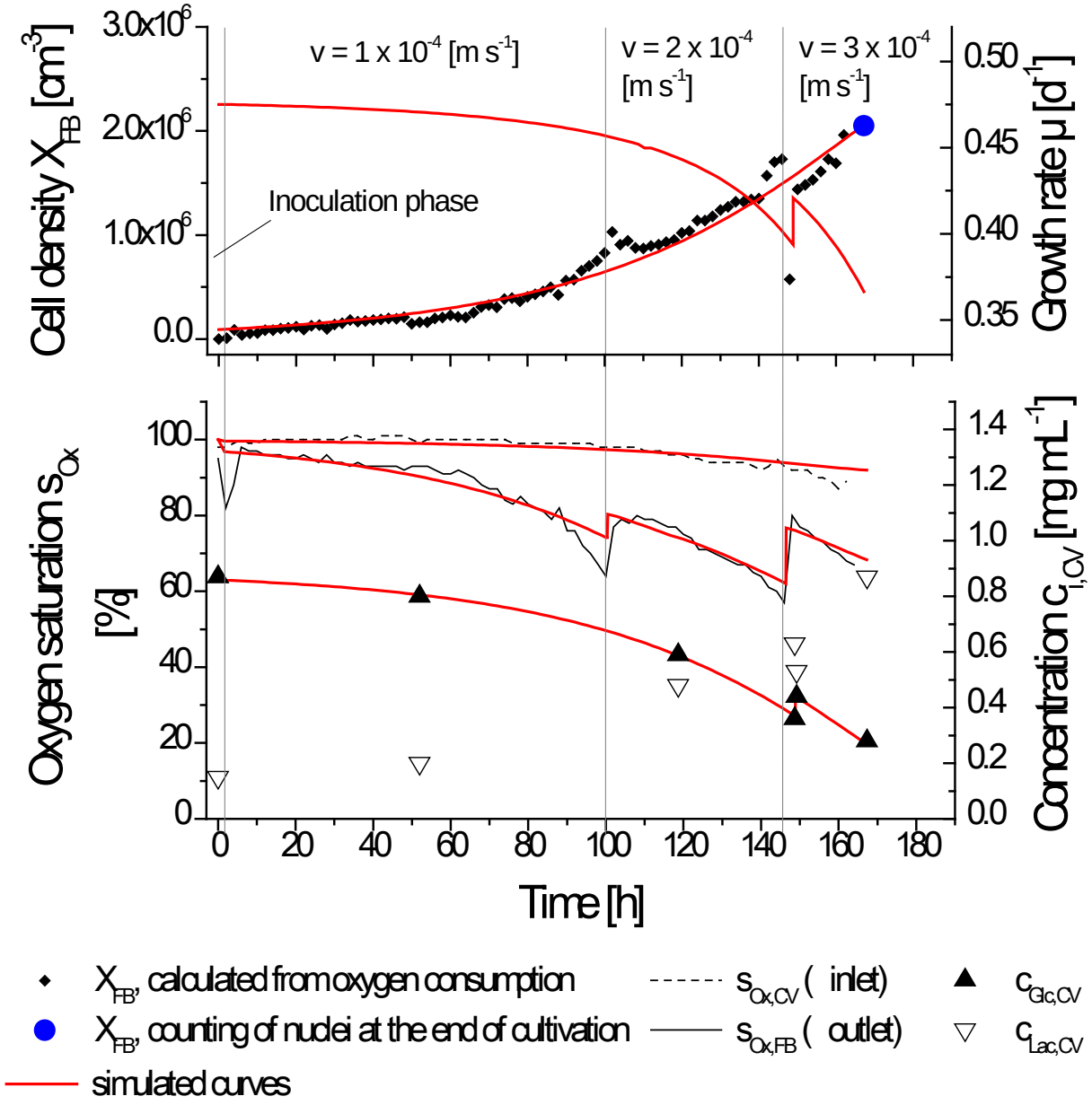
v = 1 x 10-4 [m s-1]
v = 2 x 10-4 [m s-1]
v = 3 x 10-4 [m s-1]
Inoculation phase
Cell density XFB [cm-3]
Growth rate μ [d-1]
Oxygen saturation sOx [%]
Concentration cl,CV [mg mL-1]
Time [h]
XFB, calculated from oxygen consumption
XFB, counting of nuclei at the end of cultivation
simulated curves
sOx,CV (inlet)
sOx,FB (outlet)
cGlc,CV
cLac,CV

Figure 5

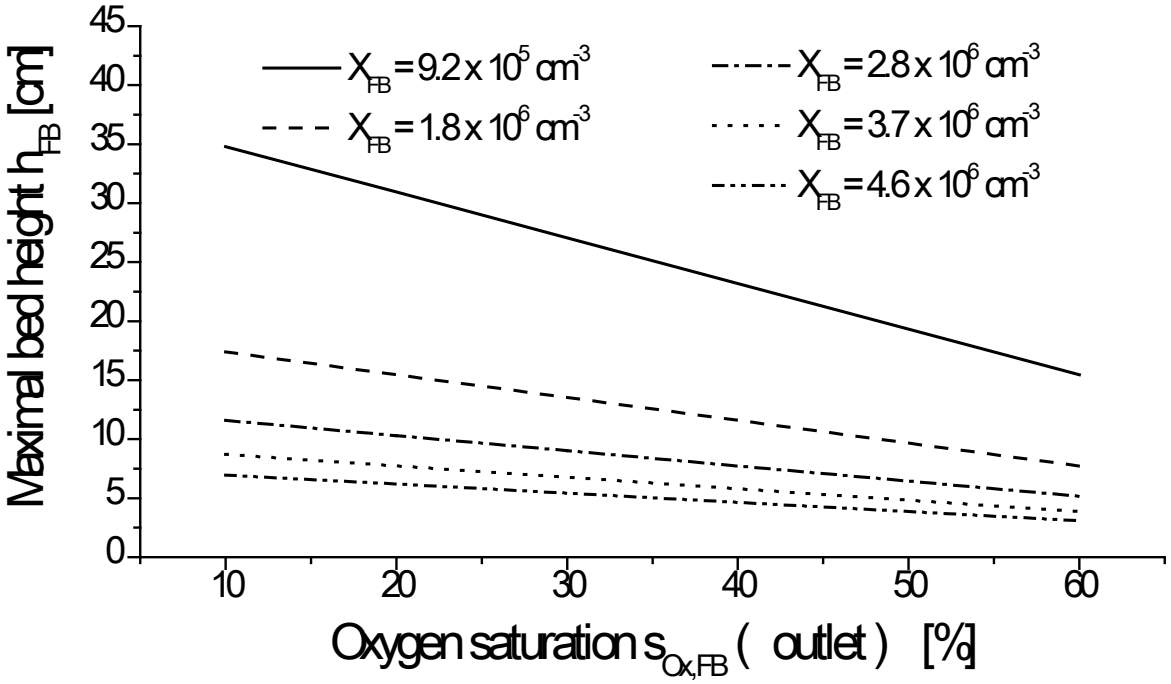
Maximal bed height h_{FB} [cm]
45
40
35
30
25
20
15
10
5
0
$X_{FB} = 9.2 \times 10^5$ cm^{-3}
$X_{FB} = 1.8 \times 10^6$ cm^{-3}
$X_{FB} = 2.8 \times 10^6$ cm^{-3}
$X_{FB} = 3.7 \times 10^6$ cm^{-3}
$X_{FB} = 4.6 \times 10^6$ cm^{-3}
10
20
30
40
50
60
Oxygen saturation $s_{Ox,FB}$ (outlet) [%]

Figure 6

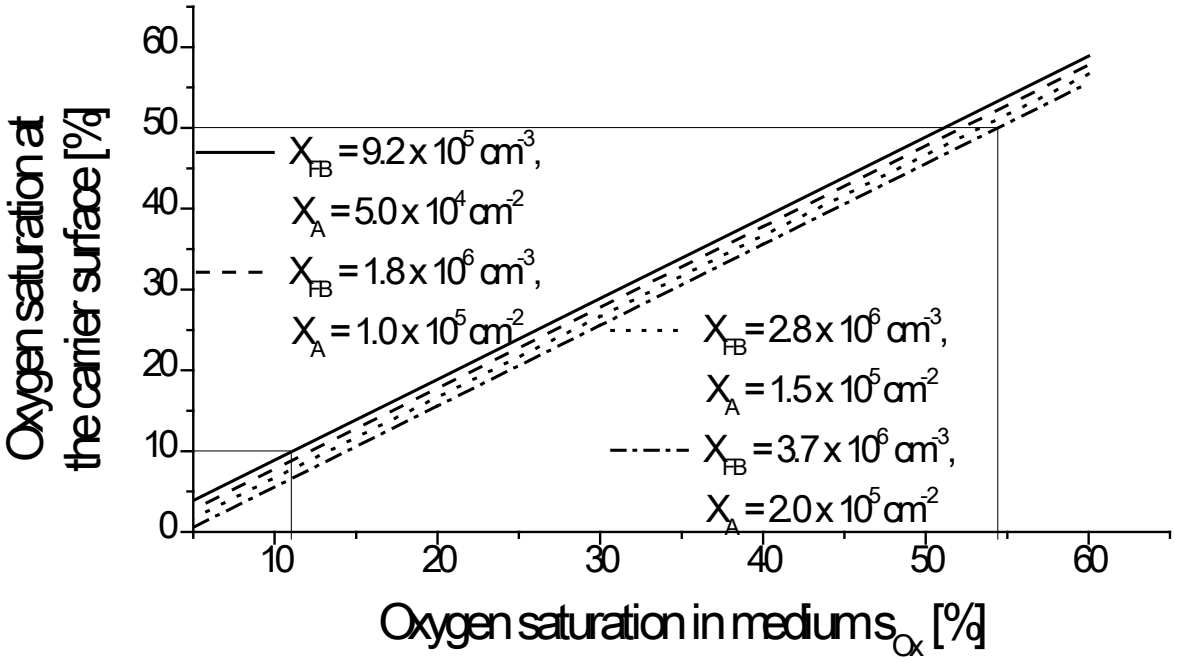
Oxygen saturation at the carrier surface [%]
Oxygen saturation in mediums s_{Ox} [%]
$X_{FB} = 9.2 \times 10^5$ cm^{-3},
$X_A = 5.0 \times 10^4$ cm^{-2}
$X_{FB} = 1.8 \times 10^6$ cm^{-3},
$X_A = 1.0 \times 10^5$ cm^{-2}
$X_{FB} = 2.8 \times 10^6$ cm^{-3},
$X_A = 1.5 \times 10^5$ cm^{-2}
$X_{FB} = 3.7 \times 10^6$ cm^{-3},
$X_A = 2.0 \times 10^5$ cm^{-2}
0
10
20
30
40
50
60

Figure 7

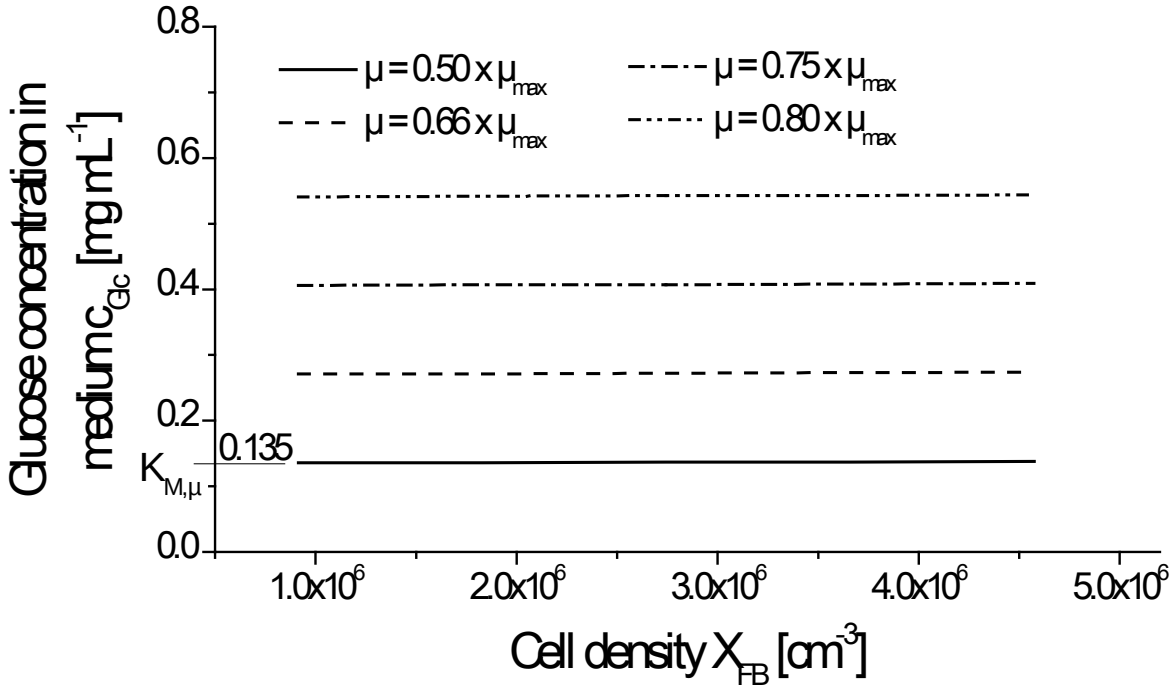
0.8
0.6
0.4
0.2
0.0
0.135
$K_{M,\mu}$
$\mu = 0.50 \times \mu_{max}$
$\mu = 0.66 \times \mu_{max}$
$\mu = 0.75 \times \mu_{max}$
$\mu = 0.80 \times \mu_{max}$
Glucose concentration in medium c_{Glc} [mg mL^{-1}]
1.0x10^6
2.0x10^6
3.0x10^6
4.0x10^6
5.0x10^6
Cell density X_{FB} [cm^{-3}]

Figure 8

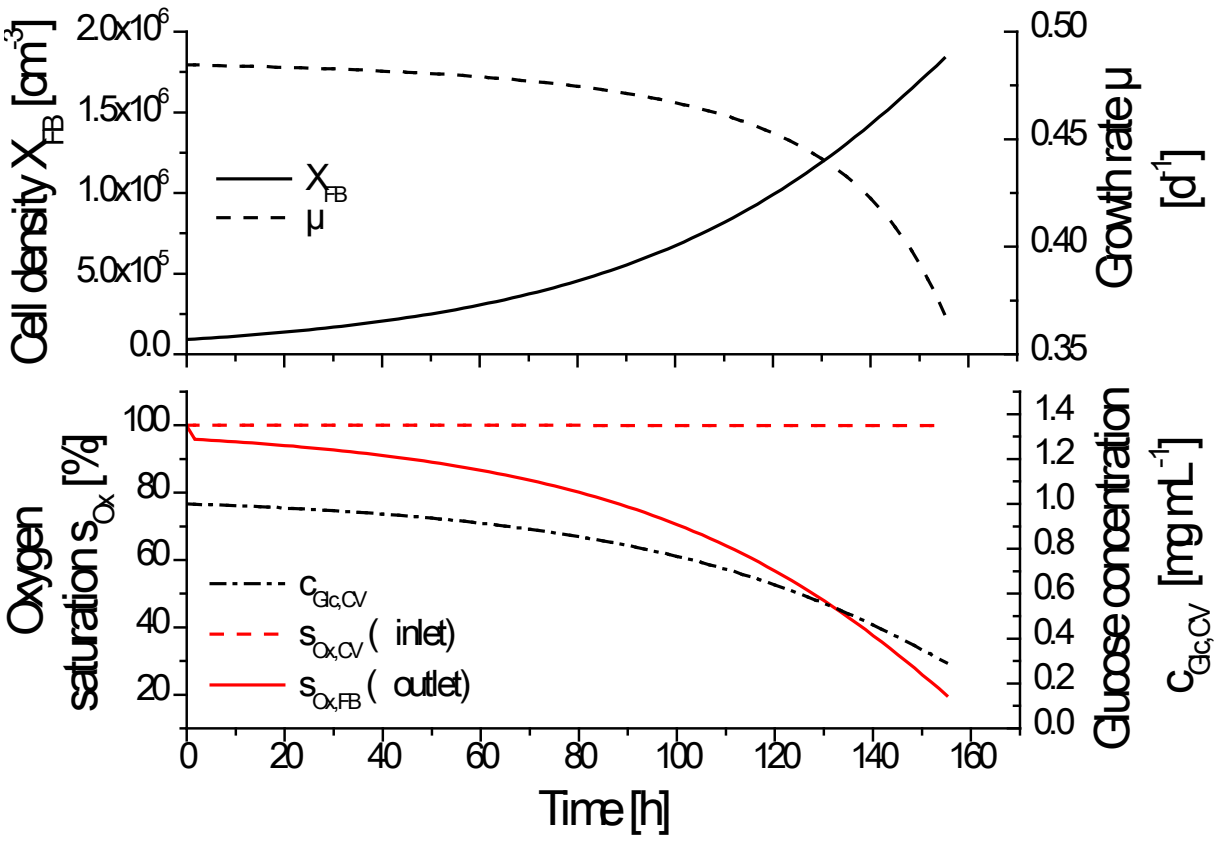
Cell density X_{FB} [cm^{-3}]
2.0x10^6
1.5x10^6
1.0x10^6
5.0x10^5
0.0
X_{FB}
μ
0.50
0.45
0.40
0.35
Growth rate μ [d^{-1}]
Oxygen saturation s_{Ox} [%]
100
80
60
40
20
$c_{Glc,CV}$
$s_{Ox,CV}$ (inlet)
$s_{Ox,FB}$ (outlet)
1.4
1.2
1.0
0.8
0.6
0.4
0.2
0.0
Glucose concentration $c_{Glc,CV}$ [mg mL^{-1}]
0
20
40
60
80
100
120
140
160
Time [h]

Figure 9

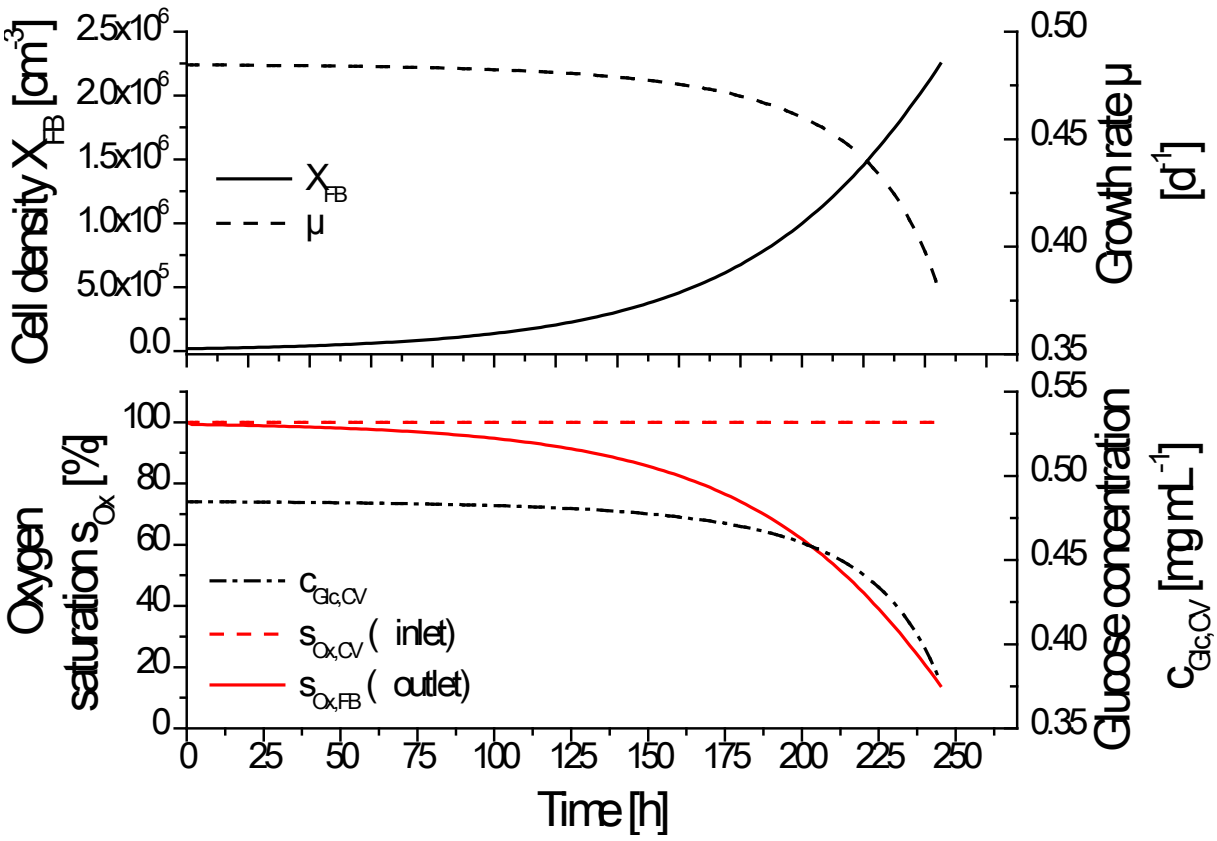
Cell density X_{FB} [cm^{-3}]
2.5x10^6
2.0x10^6
1.5x10^6
1.0x10^6
5.0x10^5
0.0
X_{FB}
μ
Growth rate μ [d^{-1}]
0.50
0.45
0.40
0.35
Oxygen saturation s_{Ox} [%]
100
80
60
40
20
0
$c_{Glc,CV}$
$s_{Ox,CV}$ (inlet)
$s_{Ox,FB}$ (outlet)
Glucose concentration $c_{Glc,CV}$ [mg mL^{-1}]
0.55
0.50
0.45
0.40
0.35
0
25
50
75
100
125
150
175
200
225
250
Time [h]

Figure 10

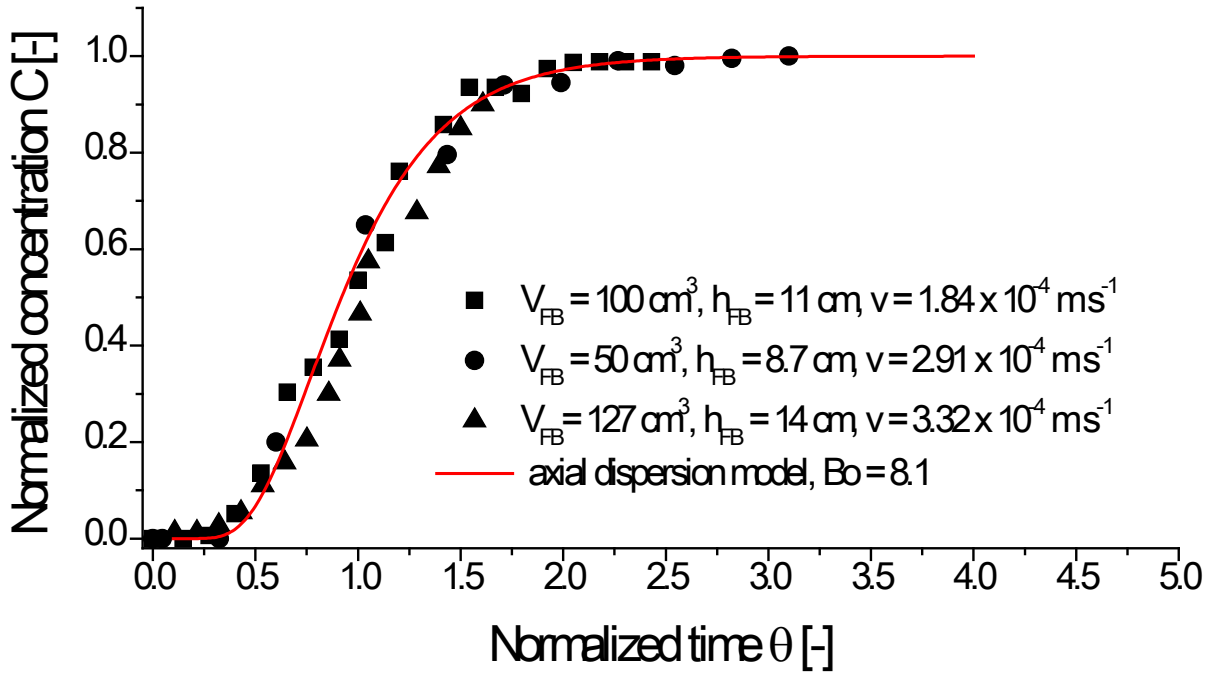
Normalized concentration C [-]
1.0
0.8
0.6
0.4
0.2
0.0
0.0
0.5
1.0
1.5
2.0
2.5
3.0
3.5
4.0
4.5
5.0
Normalized time θ [-]
V_FB = 100 cm^3, h_FB = 11 cm, v = 1.84 x 10^-4 ms^-1
V_FB = 50 cm^3, h_FB = 8.7 cm, v = 2.91 x 10^-4 ms^-1
V_FB = 127 cm^3, h_FB = 14 cm, v = 3.32 x 10^-4 ms^-1
axial dispersion model, Bo = 8.1

Figure 11

Legends

Figure 1: Illustration of the mass balances of the fixed bed and the associated conditioning vessel.

Figure 2**:** Overview to the mass transport phenomena at the carrier surface.

Figure 3: Experimental and simulated data of a hMSC-TERT cultivation in four parallel operated 14.2-cm^3 fixed-bed reactors. For calculation of the cell density from the oxygen consumption it was supposed that the cells in the reactor were 100% vital since non-vital cells get flushed out by the medium flow.

v = 2.7 x 10^{-4} m s^{-1}; V_{CV} = 1000 ml

Figure 4: Experimental and simulated data of a hMSC-TERT cultivation in a 60-cm^3 fixed-bed reactor.

v = 3.0 x 10^{-4} m s^{-1}; V_{CV} = 500 ml

Figure 5: Experimental and simulated data of a hMSC-TERT cultivation in a 300-cm^3 fixed-bed reactor.

V_{CV} = 4800 ml

Figure 6**:** Simulated maximal fixed bed height h_{FB} as a function of the cell density X_{FB} and the oxygen saturation at the outlet. A fixed superficial velocity v of 3.0 x 10^{-4} m s^{-1} and oxygen saturation at the inlet of 100%, related to normal air with 21% oxygen, was assumed.

Figure 7: Oxygen saturation at the carrier surface versus oxygen saturation in the medium for different cell densities.

q_{Ox} = 2.1 x 10^{-8} m s^{-1}; v = 3.0 x 10^{-3} m s^{-1}

Figure 8: Dependence of the glucose concentration c_{Glc} in the medium, which is necessary for maintaining certain growth rates μ, on the cell density X_{FB}. The given growth rates arises from Equation 6 by replacing the glucose concentration at the carrier surface $c_{Glc}\big|_{r=R}$ by multiples of the Monod constant $K_{M,\mu}$.

$\mu_{\max}$ = 0.55 d^{-1}; $K_{M,\mu}$ = 0.135 mg ml^{-1}; $q_{Glc,\max}$ = 1.2 x 10^{-7} mg h^{-1} $cell^{-1}$, $K_{M,q_{Glc}}$ = 1.0 mg ml^{-1}; v = 3.0 x 10^{-3} m s^{-1}

Figure 9: Simulation 1 – hMSC-TERT cultivation in production scale on 2-mm borosilicate glass spheres in a fixed-bed reactor.

n_{FB} = 4; V_{FB} = 2,905 cm^3; TR = 1.0; V_{CV} = 150 l; X_{FB}^0 = 9.15 x 10^4 cells/cm^3 (5.0 x 10^3 cells/cm^2); X_{FB}^n = 1.83 x 10^6 cells/cm^3 (1.0 x 10^5 cells/cm^2); minimal oxygen saturation at the outlet $s_{Ox,FB}$ = 20%; v = 3.0 x 10^{-4} m s^{-1}

Figure 10: Simulation 4 – hMSC-TERT cultivation in production scale on 2-mm borosilicate glass spheres in a fixed-bed reactor.

n_{FB} = 6; V_{FB} = 1,946 cm^3; TR = 1.0; V_{CV} = 200 l; X_{FB}^0 = 1.83 x 10^4 cells/cm^3 (1.0 x 10^3 cells/cm^2); X_{FB}^n = 1.83 x 10^6 cells/cm^3 (1.0 x 10^5 cells/cm^2); minimal oxygen saturation at the outlet $s_{Ox,FB}$ = 30%; v = 3.0 x 10^{-4} m s^{-1}

Figure 11: Simulated and experimental step response of fixed-bed reactors consisted of 2-mm non-porous glass spheres.

Tables

Table 1: Performed hMSC-TERT cultivations in fixed bed bioreactors at different scales.

Fixed bed volume V_{FB} [cm^3]	Growth surface A_{FB} [cm^2]	Inoculated cell density [cm^{-2}]	Medium volume V_{CV} [mL]	Superficial velocity v [$m\ s^{-1}$]	Medium changes [h]	Cultivation time [h]
4 x 14.2	4 x 260	10,000	1,000	2.65 x 10^{-4}	115	135
60	1098	7,000	500	3.0 x 10^{-4}	-	168
300	5490	10,000	4,800	(0.8– 3.3) x 10^{-4}	149	167

Table 2: Results of the hMSC-TERT cultivation in 2-mm borosilicate glass spheres comprising fixed-bed reactors – simplified calculations (see part A of this publication) [3].

Parameter	Units	V_{FB} = 4 x 14.2 cm^3	V_{FB} = 60 cm^3	V_{FB} = 300 cm^3
Passage number	-	68	71	84
Mean growth rate μ_{m}	[d^{-1}]	0.60 ± 0.02	0.49 ± 0.04	0.42 ± 0.02
Mean glucose consumption rate $q_{Glc,\mathrm{m}}$	[mg h^{-1} cell^{-1}]	(7.65 ± 0.3) x 10^{-8}	(6.80 ± 0.43) x 10^{-8}	(9.50 ± 0.27) x 10^{-8}
Oxygen consumption rate q_{Ox}	[mg h^{-1} cell^{-1}]	2.03 x 10^{-8}	2.06 x 10^{-8}	1.08 x 10^{-8}

Table 3: Parameters and coefficients used for modeling of the fixed bed cultivation. Kinetic parameters are given in Table 5.

Parameter		Units	Value	Reference	Remarks
c_{Glc}^{0}	Initial glucose concentration	[mg L^{-1}]	1000	Biochrom	EMEM
c_{Ox}^{*}	Maximal oxygen saturation	[mg L^{-1}]	6,88	[16]	37°C, atmospheric pressure, 21% O_2
D_M	Diffusion coefficient for glucose	[cm^2 s^{-1}]	7.0 x 10^{-6}	[17]	in water, 30°C
D_M	Diffusion coefficient for oxygen	[cm^2 s^{-1}]	3.24 x 10^{-5}	[18]	in water, 40°C
		[cm^2 s^{-1}]	1.97 x 10^{-5}	[18]	in water, 30°C
		[cm^2 s^{-1}]	2.86 x 10^{-5}	interpolated	37°C
ε	Porosity	[-]	0.39	experimental	randomly packed bed of monodisperse spheres
η	Dynamic viscosity of medium	[Pa s]	7.4 x 10^{-4}	[19]	DMEM + 5 % FCS , 37°C
		[Pa s]	7.8 x 10^{-4}	[19]	DMEM + 25 % FCS , 37°C
		[Pa s]	7.5 x 10^{-4}	interpolated	DMEM + 10 % FCS , 37°C
ρ	Density of medium	[kg m^{-3}]	1003	[19]	DMEM, 37°C
Bo	Bodenstein number	[-]	8.1	experimental	see appendix

Table 4: Range of growth and consumption rates of animal cells.

Parameter	Value	Reference
Growth rate μ [d^{-1}]	0.23 – 1.56	[7, 20-25]
Glucose consumption rate q_{Glc} [mg h^{-1} $cell^{-1}$]	(0.9 – 1.6) x 10^{-7}	[7, 26-32]
Oxygen consumption rate q_{Ox} [mg h^{-1} $cell^{-1}$]	(1.1 – 3.2) x 10^{-8}	[33-37]

Table 5: Growth and consumption kinetics of hMSC-TERT during the cultivations in 2-mm borosilicate glass spheres comprising fixed-bed reactors and 6-well cell culture plates. Bold-faced values were determined by fitting of the model parameters to the experimental data. Underlined kinetic parameter were used for scale up considerations.

Reference	Units	V_{FB} = 4 x 14.2 cm^3	V_{FB} = 60 cm^3	V_{FB} = 300 cm^3	6-Well [3]
Cultivation time	[h]	135	168	167,3	173,5
End cell density X_{FB}^{n}	[cm^{-2}] [cm^{-3}]	(1.60 ± 0.06) x 10^5 (2.93 ± 0.11) x 10^6	9.56 x 10^4 1.75 x 10^6	1.12 x 10^5 2.05 x 10^6	6.5 x 10^4 *
Passage number	-	68	71	84	68
Superficial velocity v	[m s-1]	2.7 x 10^{-4}	3.0 x 10^{-4}	(0.8 – 3.3) x 10^{-4}	0
Axial dispersion coefficient D_{ax} (Bo = 8.1)	[m^2 s^{-1}]	1.47 x 10^{-6}	3.89 x 10^{-6}	3.18 x 10^{-6}	-
Initial cell density X_A^0 and X_{FB}^0	[cm^{-2}] [cm^{-3}]	**5.50 x 10^3** **9.15 x 10^4**	**3.50 x 10^3** **6.40 x 10^4**	**5.00 x 10^3** **9.12 x 10^4**	5.00 x 10^3
Maximal growth rate $\mu_{\max}$	[d^{-1}]	**0.69**	**0.58**	**<u>0.55</u>**	0.66 ± 0.02
Monod constant $K_{M,\mu}$	[mg mL^{-1}]	**0.14**	**0.16**	**<u>0.14</u>**	0.14 ± 0.03
Maximal glucose consumption rate $q_{Glc,\max}$	[mg h^{-1} cell^{-1}]	**8.0 x 10^{-8}**	**9.15 x 10^{-8}**	**<u>1.18 x 10^{-7}</u>**	(7.65 ± 1.11) x 10^{-8}
Monod constant $K_{M,q_{Glc}}$	[mg mL^{-1}]	**0.15**	**0.16**	**<u>0.10</u>**	0.16 ± 0.06
Oxygen consumption rate q_{Ox}	[mg h^{-1} cell^{-1}]	**<u>2.14 x 10^{-8}</u>**	**2.05 x 10^{-8}**	**0.98 x 10^{-8} (0 - 100 h)** **1.11 x 10^{-8} (100 - 146 h)** **1.62 x 10^{-8} (146 - 167 h)**	-

$k_l a$	[h^{-1}]	**2.15**	**1.6**	**2.22**	-

* Glucose limitation

** Appendix

Table 6: Numbers and volumes of parallel operated fixed beds needed for the cultivation of twenty billion cells.

	Thickness ratio = 1		Thickness ratio = 2		Thickness ratio = 3		
Target cell density X_{FB}^{n} $\left(X_{A}^{n}\right)$ [cm^{-3}] ([cm^{-2}])	Fixed bed volume V_{FB} [cm^3]	Number of fixed beds n_{FB}	Fixed bed volume V_{FB} [cm^3]	Number of fixed beds n_{FB}	Fixed bed volume V_{FB} [cm^3]	Number of fixed beds n_{FB}	Total fixed bed volume for 2×10^{10} cells [cm^3]
Outlet oxygen saturation $s_{Ox,FB}$ = 20%							
9.15×10^5 (5.0×10^4)	23,241	0.9	5,810	3.8	2,582	8.5	21,858
1.83×10^6 (1.0×10^5)	2,905	3.8	726	15.1	323	33.9	10,929
2.75×10^6 (1.5×10^5)	861	8.5	215	33.9	96	76.2	7,286
3.66×10^6 (2.0×10^5)	363	15.1	91	60.2	40	135.4	5,464
Outlet oxygen saturation $s_{Ox,FB}$ = 30%							
9.15×10^5 (5.0×10^4)	15,570	1.4	3.892	5.6	1730	12.6	21,858
1.83×10^6 (1.0×10^5)	1,946	5.6	487	22.5	216	50.5	10,929
2.75×10^6 (1.5×10^5)	577	12.6	144	50.5	64	113.7	7,286
3.66×10^6 (2.0×10^5)	243	22.5	61	89.9	27	202.2	5,464
Outlet oxygen saturation $s_{Ox,FB}$ = 40%							
9.15×10^5 (5.0×10^4)	9,805	2.2	2.451	8.9	1.089	20.1	21,858
1.83×10^6 (1.0×10^5)	1,226	8.9	306	35.7	136	80.3	10,929
2.75×10^6 (1.5×10^5)	363	20.1	91	80.3	40	180.6	7,286
3.66×10^6 (2.0×10^5)	153	35.7	38	142.7	17	321.0	5,464

Table 7: Performed simulations of the hMSC-TERT expansion process based on fixed-bed reactors with 2-mm borosilicate glass spheres. Target cell number = 2.0 x 10^{10} cells

Simulation	1	2	3	4
Initial cell density X_{FB}^{0} [cm^{-3}]	9.15 x 10^{4}	9.15 x 10^{4}	4.58 x 10^{4}	1.83 x 10^{4}
Target cell density X_{FB}^{n} [cm^{-3}]	1.83 x 10^{6}	1.83 x 10^{6}	9.15 x 10^{5}	1.83 x 10^{6}
Outlet oxygen saturation $s_{Ox,FB}$ by achieving the target cell density [%]	20	30	20	30
Fixed bed height h_{FB} [cm]	15.47	13.53	30.95	13.53
Fixed bed volume of a single reactor V_{FB} [cm^{3}]	2,905	1,946	23,241	1,946
Number of fixed-bed reactors n_{FB} [-] (calculated)	4 (3.76)	6 (5.6)	1 (0.94)	6 (5.6)
Total fixed bed volume [cm^{3}]	11,620	11,676	23,241	11,676
Total fixed bed volume needed for the cultivation of 2 x 10^{10} cells [cm^{3}]	10,929	10,929	21,858	10,929
Medium volume V_{CV} [L]	150	125	150	200
Axial dispersion coefficient D_{ax} [$m^{2}\,s^{-1}$]	5.73 x 10^{-6}	5.01 x 10^{-6}	1.14 x 10^{-5}	5.01 x 10^{-6}
Superficial velocity v [$m\,s^{-1}$]	3.0 x 10^{-4}			
Oxygen saturation at the inlet $s_{Ox,CV}$ [%]	100			
Thickness ratio TR [-]	1.0			

Table 8: Results of the simulations of hMSC-TERT cultivations in fixed-bed reactors consisting of 2-mm borosilicate glass spheres. The data are related to the point of reaching the target cell density X_{FB}^{n}.

Simulation	1	2	3	4
Time until reaching the target cell density [h]	155.0	158.8	154.6	232.8
Total cell number [-]	2.13 x 10^{10}	2.14 x 10^{10}	2.13 x 10^{10}	2.14 x 10^{10}
Glucose concentration in the conditioning vessel $c_{Glc,CV}$ [mg mL^{-1}]	0.292	0.143	0.314	0.438
Glucose concentration at the outlet $c_{Glc,FB}$ [mg mL^{-1}]	0.270	0.128	0.292	0.422
Glucose concentration at the carrier surface $c_{Glc}\big\vert_{r=R}$ (upper fixed bed area) [mg ml^{-1}]	0.269	0.127	0.291	0.421
Oxygen saturation at the outlet $s_{Ox,FB}$ [%]	20.0	30.0	20.0	30.0
Oxygen saturation at the carrier surface $s_{Ox}\big\vert_{r=R}$ (upper fixed bed area) [%]	17.8	27.8	18.9	27.8
Growth rate μ [d^{-1}]	0.37	0.27	0.38	0.42

Table 9: Overview of the fixed bed dimensions and superficial velocities used for determination of the axial dispersion coefficient.

Fixed bed volume V_{FB} [cm^3]	Sphere diameter d [mm]	Fixed bed height h_{FB} [cm]	Fixed bed diameter d_{FB} [cm]	Superficial velocity v [m s^{-1}]
50	2.0	8.7	2.7	2.91×10^{-4}
100	2.0	11.9	3.4	1.84×10^{-4}
127	2.0	14.0	3.4	3.32×10^{-4}

References

[1] **Heile, A.M.B., C. Wallrapp, P.M. Klinge, A. Samii, M. Kassem, G. Silverberg and T. Brinker.** ***Cerebral Q1 transplantation of encapsulated mesenchymal stem cells improves cellular pathology after experimental traumatic brain injury.*** **Neurosci Lett. 2009; 463: 176-181**

[2] **Vijaa, L., D. Fargec, J.F. Gautierb, P. Vexiaub, C. Dumitrached, A. Bourgaritc, F. Verrecchiaa and J. Larghero.** ***Mesenchymal stem cells: Stem cell therapy perspectives for type 1 diabetes*** **2009; 35: 85-93**

[3] **Weber, C., D. Freimark, R. Poertner, P. Pino-Grace, S. Pohl, C. Wallrapp, P. Geigle and P. Czermak.** ***Expansion of human mesenchymal stem cells in a fixed-bed bioreactors system - Part A: Inoculation, cultivation, and harvesting procedures.*** **Int J Artif Organs 2010;**

[4] **Weber, C., S. Pohl, R. Poertner, P. Pino-Grace, D. Freimark, C. Wallrapp, P. Geigle and P. Czermak,** ***Production process for stem cell-based therapeutic implants - Expansion of the production cell line and cultivation of encapsulated cells*****. Advances in Biochemical Engineering/Biotechnology, eds.: C. Kasper, M. van Griensven und R. Poertner, Volume: , , in press. 2010, Berlin: Springer.**

[5] **Simonsen, J.L., C. Rosada, N. Serakinci, J. Justesen, K. Stenderup, S.I.S. Rattan, T.G. Jensen and M. Kassem.** ***Telomerase expression extends the proliferative life-span and maintains the osteogenic potential of human bone marrow stromal cells.*** **Nat Biotechnol. 2002; 20: 592-596**

[6] **Weber, C., S. Pohl, R. Pörtner, C. Wallrapp, M. Kassem, P. Geigle and P. Czermak.** ***Cultivation and differentiation of encapsulated hMSC-TERT in a disposable small-scale syringe-like fixed bed reactor.*** **Open Biomed Eng J. 2007; 1: 64-70**

[7] **Higuera, G., D. Schop, F. Janssen, R. van Dijkhuizen-Radersma, T. van Boxtel and C.A. van Blitterswijk.** ***Quantifying in vitro growth and metabolism kinetics of human mesenchymal stem cells using a mathematical model.*** **Tissue Eng Part A. 2009; 15: 2653-2663**

[8] **Karabelas, A.J., T.H. Wegner and T.J. Hanratty.** ***Use of asymptotic relations to correlate mass transfer data in packed beds*** **Chem Eng Sci. 1971; 26: 1581-1589**

[9] **Hung, S.C., R.R. Pochampally, S.C. Hsu, C. Sanchez, S.C. Chen, J. Spees and D.J. Prockop.** ***Short-term exposure of multipotent stromal cells to low oxygen increases their expression of CX3CR1 and CXCR4 and their engraftment in vivo.*** **PLoS ONE. 2007; 2: e416**

[10] **Fehrer, C., R. Brunauer, G. Laschober, H. Unterluggauer, S. Reitinger and F. Kloss.** ***Reduced oxygen tension attenuates differentiation capacity of human mesenchymal stem cells and prolongs their lifespan.*** **Aging Cell. 2007; 6: 745-757**

[11] **Krinner, A., M. Zscharnack, A. Bader, D. Drasdo and J. Galle.** ***Impact of oxygen environment on mesenchymal stem cell expansion and chondrogenic differentiation.*** **Cell Prolif. 2009; 42: 471-484**

[12] **Grayson, W.L., F. Zhao, R. Izadpanah, B. Bunnell and T. Ma.** ***Effects of hypoxia on human mesenchymal stem cell expansion and plasticity in 3D constructs.*** **J Cell Physiol. 2006; 207: 331-339**

[13] **Ma, T., W.L. Grayson, M. Fröhlich and G. Vunjak-Novakovic.** ***Hypoxia and stem cell-based engineering of mesenchymal tissues.*** **Biotechnol Prog. 2009; 25: 32-42**

[14] **Weber, C., S. Gokorsch and P. Czermak.** ***Expansion and chondrogenic differentiation of human mesenchymal stem cells.*** **Int J Artif Organs. 2007; 30: 611-618**

[15] **Weber, C., S. Pohl, R. Pörtner, C. Wallrapp, M. Kassem, P. Geigle and P. Czermak.** ***Expansion and harvesting of hMSC-TERT.*** **Open Biomed Eng J. 2007; 1: 38-46**

[16] **Pörtner, R. and M. Koop.** ***A model for oxygen supply in fixed bed reactors with immobilized hybridoma cells.*** **Bioprocess Biosyst Eng. 1997; 17: 269-275**

[17] **Venâncio, A. and J.A. Teixeira.** ***Characterization of sugar diffusion coefficients in alginate membranes.*** **Biotechnol Techn. 1997; 11: 183-186**

[18] **Weast, R.C.,** ***CRC handbook of chemistry and physics.*** **1978, Florida: CRC Press.**

[19] **Croughan, M.S., E.S. Sayre and D.I.C. Wang.** ***Viscous reduction of turbulent damage in animal cell culture.*** **Biotechnol Bioeng. 1988; 33: 862-872**

[20] **Lonergan, T., C. Brenner and B. Bavister.** ***Differentiation-related changes in mitochondrial properties as indicators of stem cell competence.*** **J Cell Physiol. 2006; 208: 149-153**

[21] **Conget, P.A. and J.J. Minguell.** ***Phenotypical and functional properties of human bone marrow mesenchymal progenitor cells.*** **J Cell Physiol. 1999; 181: 67-73**

[22] **Guo, Z., J. Yang, X. Liu, X. Li, C. Hou, P.H. Tang and N. Mao.** ***Biological features of mesenchymal stem cells from human bone marrow.*** **Chin Med J. 2001; 114: 950-953**

[23] **Liu, Y.-H., J.-X. Bi, A.-P. Zeng and J.-Q. Yuan.** ***A simple kinetic model for myeloma cell culture with consideration of lysine limitation.*** **Bioprocess Biosyst Eng. 2008; 31: 569-577**

[24] **Soukup, T., J. Mokrý, J. Karbanová, R. Pytlík, P. Suchomel and L. Kučerová.** ***Mesenchymal stem cells isolated from human bone marrow: cultivation, phenotypic analysis and changes in proliferation kinetics.*** **Acta Med (Hradec Kralove). 2006; 49: 27-33**

[25] **Amit, M., M.K. Carpenter, M.S. Inokuma, C.P. Chiu and J.A. Thomson.** ***Clonally derived human embryonic stem cell lines maintain pluripotency and proliferative potential for prolonged periods of pulture.*** **Dev Biol. 2000; 227: 271–278**

[26] **Abranches, E., E. Bekman, D. Henrique and J.M.S. Cabral.** ***Expansion of mouse embryonic stem cells on microcarriers.*** **Biotechnol Bioeng. 2006; 96: 1211-1221**

[27] **Breguet, V., R.I. Gugerli, U. von Stockar and I.W. Marison.** ***CHO immobilization in alginate/poly-L-lysine microcapsules: an understanding of potential and limitations.*** **Cytotechnology. 2007; 53: 81–93**

[28] **Shirai, Y., K. Hashimoto and H. Takamatsu.** ***Growth kinetics of Hybridoma cells in high density culture.*** **J Ferment Bioeng. 1992; 73: 159-165**

[29] **Schop, D., F.W. Janssen, E. Borgart, J.D. de Bruijn and R. van Dijkhuizen-Radersma.** ***Expansion of mesenchymal stem cells using a microcarrier-based cultivation system: growth and metabolism.*** **J Tissue Eng Regen Med. 2008; 2: 126-135**

[30] **Boren, J., M. Cascante, S. Marin, B. Comın-Anduix, J.J. Centelles, S. Lim, S. Bassilian, S. Ahmed, W.N.P. Lee and L.G. Boros.** ***Gleevec (STI571) influences metabolic enzyme activities and glucose carbon flow toward nucleic acid and fatty acid synthesis in myeloid tumor cells.*** **J Biol Chem. 2001; 276: 37747–37753**

[31] **Frahm, B., P. Lane, H. Atzert, A. Munack, M. Hoffmann, V.C. Hass and R. Pörtner.** ***Adaptive, model-based control by the open-loop-feedback-optimal (OLFO) controller for the effective fed-batch cultivation of hybridoma cells.*** **Biotechnol Prog. 2002; 18: 1095-1103**

[32] **Lubiniecki, A.S., *Large-scale mammalian cell culture technology*. 1990: Marcel Dekker Inc.**

[33] **Peng, C.A. and B.A. Palson. *Determination of specific oxygen uptake rates in human hematopoietic cultures and implications for bioreactor design.* Ann Biomed Eng. 1996; 24: 373-381**

[34] **Acevedo, C.A., C. Weinstein-Oppenheimer, D.I. Brown, H. Huebner, R. Buchholz and M.E. Young. *A mathematical model for the design of fibrin microcapsules with skin cells.* Bioprocess Biosyst Eng. 2008; 32: 341-351**

[35] **De Leòn, A., H. Mayani and O.T. Ramırez. *Design, characterization and application of a minibioreactor for the culture of human hematopoietic cells under controlled conditions.* Cytotechnology. 1998; 28: 127-138**

[36] **Youn, B.S., A. Sen and L.A. Behie. *Scale-up of breast cancer stem cell aggregate cultures to suspension bioreactors.* Biotechnol Prog. 2006; 22: 801-810**

[37] **Shirai, Y., K. Hashimoto, H. Yamaji and H. Kawahara. *Oxygen uptake rate of immobilized growing hybridoma cells.* Appl Microbiol Biotechnol. 1988; 29: 113-118**